Melatonin enhances neural stem cell differentiation and engraftment by increasing mitochondrial function.

Miguel Mendivil-Perez[1], Viviana Soto-Mercado[1], Ana Guerra-Librero[2], Beatriz I Fernandez-Gil[2], Javier Florido[2], Ying-Qiang Shen[2], Miguel A Tejada[2], Vivian Capilla-Gonzalez[3,4], Iryna Rusanova[2,6], José M Garcia-Verdugo[3], Darío Acuña-Castroviejo[2,5,6], Luis Carlos López[2,5,6], Carlos Velez-Pardo[1], Marlene Jimenez-Del-Rio[1], José M Ferrer[5], Germaine Escames[2,5,6]

[1]Medical Research Center, Faculty of Medicine, Universidad de Antioquia, Medellin, Colombia.

[2]Medical Research Institute, Health Sciences Technology Park, Universidad de Granada, Granada, Spain.

[3] Cavanilles Institute of Biodiversity and Evolutionary Biology, Universitat de Valencia, Valencia, Spain

[4] Andalusian Center for Molecular Biology and Regenerative Medicine (CABIMER), Seville, Spain

[5] Department of Physiology, Faculty of Medicine, Universidad de Granada, Granada, Spain.

[6] CIBERFES, Biosanitary Research Institute, Complejo Hospitalario de Granada, 18016 Granada, Spain

Running title: Pharmacological melatonin concentrations induce NSC differentiation

Keywords: melatonin, neural stem cells, mitochondria, transplant, Parkinson's disease, Alzheimer's disease, oxidative stress.

Abstract

Neural stem cells (NSCs) are regarded as a promising therapeutic approach to protecting and restoring damaged neurons in neurodegenerative diseases (NDs) such as Parkinson's disease and Alzheimer's disease (PD and AD, respectively). However, new research suggests that

NSC differentiation is required to make this strategy effective. Several studies have demonstrated that melatonin increases mature neuronal markers, which reflects NSC differentiation into neurons. Nevertheless, the possible involvement of mitochondria in the effects of melatonin during NSC differentiation has not yet been fully established. We therefore tested the impact of melatonin on NSC proliferation and differentiation in an attempt to determine whether these actions depend on modulating mitochondrial activity. We measured proliferation and differentiation markers, mitochondrial structural and functional parameters as well as oxidative stress indicators and also evaluated cell transplant engraftment. This enabled us to show that melatonin (25 μM) induces NSC differentiation into oligodendrocytes and neurons. These effects depend on increased mitochondrial

mass/DNA/complexes, mitochondrial respiration and membrane potential as well as ATP synthesis in NSCs. It is also interesting to note that melatonin prevented oxidative stress caused by high levels of mitochondrial activity. Finally, we found that melatonin enriches NSC engraftment in the ND mouse model following transplantation. We concluded that a combined therapy involving transplantation of NSCs pre-treated with pharmacological doses of melatonin could efficiently restore neuronal cell populations in PD and AD mouse models depending on mitochondrial activity promotion.

1. INTRODUCTION

Neurodegenerative diseases (NDs) are characterized by a progressive loss of neuronal subtypes in the brain. The best known examples of neuron degeneration are Parkinson's disease (PD) and Alzheimer's disease (AD). PD is mainly characterized by a degeneration of nigrostriatal dopaminergic neurons, leading to decreased tyrosine hydroxylase (TH) in the midbrain. Dopamine (DA) levels in the brain are consequently reduced, which results in typical motor symptoms such as bradykinesia, rigidity and resting tremors [1]. On the other hand, AD is clinically characterized by a slowly progressive decline in learning and memory performance caused by neuron loss, leading to gross cerebral atrophy. This atrophy is

produced by the formation of extracellular plaques of neuritic amyloid-β and intracellular tau protein aggregates called neurofibrillary tangles [2].

Although the aim of current therapies is to slow down or halt the progression of PD and AD, a substantial number of neurons have been found to have already died at the clinical diagnosis stage [3,4]. Thus, it is crucial to develop new therapeutic interventions focused on restoring these lost neural populations. Recently, transplantation of human neural stem cells (NSCs) has been proposed as a promising therapy for NDs [5]. NSCs are multipotent cells present in developing and adult brains which can differentiate into astrocytes, neurons and oligodendrocytes [6]. In the adult brain, NSCs reside in neurogenic niches, such as the subventricular zone (SVZ) and subgranular zone (SGZ), in the dentate gyrus of the hippocampus [7]. Given that NSCs in the SVZ are constantly involved in neurogenesis and gliogenesis under both normal and pathological conditions [8,9], NSC-based therapy is considered to be a promising therapeutic approach to protecting and restoring damaged neurons [10]. In this regard, further research needs to be carried out to ensure that NSC differentiation for cellular restoration in PD and AD is successful.

Differentiated neurons are known to require large amounts of adenosine triphosphate (ATP) to maintain cell membrane ionic gradients and neurotransmission [11]. ATP is mainly generated by the oxidative metabolism, which explains why neurons critically depend on mitochondrial function [12]. Previous studies have shown that neuronal maturation is also dependent on oxidative metabolism [13] and, more specifically, that mitochondrial stability is critical for the successful differentiation of SVZ NSCs [14]. It is therefore important to determine whether molecules targeting mitochondrial activity improve neuronal maturation of SVZ NSCs as part of a viable therapy for PD and AD.

Melatonin (N-acetyl-5-methoxytryptamine) is a hormone which is ubiquitously secreted in the body. In mammals, melatonin is critical for physiological functions such as the circadian cycle, pubertal development and seasonal adaptation [15]. At the molecular level,

melatonin is associated with apoptosis, metastasis, angiogenesis as well as inflammatory pathways [16,17] and melatonin and its metabolites are strongly linked to antioxidant responses [18,19] due to its association with the prevention of neuronal cell death in PD [20,21] and AD [22,23] models. Several studies have also shown that melatonin promotes SVZ-NSC neurogenesis by increasing the expression of mature neuron markers, such as β-III- tubulin (Tuj-1) and TH, and by reducing the expression of the astrocytic marker glial fibrillary acidic protein (GFAP)[24-26]. Interestingly, some experimental evidence shows that mitochondria are the principal intracellular target of melatonin [27-29]. Indeed, melatonin is recognized as a possible regulator of the mitochondrial function by maintaining the efficiency of oxidative phosphorylation and ATP synthesis and by increasing the activity of respiratory complexes [30-32]. In addition, melatonin regulation may prevent damage to mitochondrial respiration [33]. Despite these advances, the possible role played by melatonin at the mitochondrial level during SVZ-NSC differentiation has not been fully established. Thus, the aim of this study was to examine the effects of melatonin on the proliferation and differentiation of NSCs derived from the SVZ of adult mice and to determine whether these effects depend on mitochondrial activity. Finally, we evaluated the impact of the transplantation of melatonin-treated NSCs on tissue regeneration in PD and AD mouse models. Our results suggest that a combined therapy involving the transplant of NSCs pre-treated with pharmacological doses of melatonin might, depending on the effect of mitochondrial activity promotion, effectively restore neuronal populations in PD and AD patients.

2. MATERIALS AND METHODS

2.1. Animals

All experiments were conducted in accordance with the norms of the University of Granada's Ethical Committee; the Spanish Protection Guide for Animal Experimentation (R.D. 53/2013) and the European Convention for the Protection of Vertebrate Animals used for Experimental and Other Scientific Purposes (ETS # 123). Wild-type C57BL/6 male mice

provided by Harland Laboratories (Barcelona, Spain) and transgenic Alzheimer mice provided by the Jackson Laboratories (Chicago, USA) were housed in clear plastic cages (four mice per cage) at the University of Granada's facility in a specific pathogen-free barrier zone subjected to a controlled 12 h light/dark cycle, with lights turned on at 08:00 h, at a constant room temperature (22 °C ± 1 °C). The mice were fed *ad libitum* and had free access to water. The PD mouse model was obtained using 10 doses of 1-methyl-4-phenyl-1,2,3,6-tetrahydropyridine (MPTP) (25 mg/kg) and probenecid (250 mg/kg) over 5 weeks, as indicated in a previous study [34]. For the AD mouse model, we used B6C3-Tg(APPswe,PSEN1dE9)85Dbo/Mmjax transgenic male mice. These double transgenic mice express a chimeric mouse/human amyloid precursor protein (Mo/HuAPP695swe) and a mutant human presenilin 1 (PS1-dE9), both directed at central nervous system (CNS) neurons. Both of these mutations are associated with early-onset Alzheimer's disease. The Mo/HuAPP695swe transgene enables mice to secrete human amyloid β peptides [35].

2.2. SVZ dissection, neurosphere cultures and differentiation

We used 3-month-old mice for the purposes of SVZ dissection and the neurosphere culture. The SVZ was dissected from 2-mm-thick coronal slices, anteriorly defined by the presence of the anterior commissure and posteriorly defined by the rostral opening of the third ventricle. A strip of tissue (2-4 mm long) was cut along the lateral wall of the lateral ventricle from the region below the corpus callosum to the ventral tip of the lateral ventricle, as described in a previous study [36]. Cells were collected from the SVZ dissected from wild-type mice in Petri dishes containing phosphate saline buffer (PBS). After digestion with papain, the cells were dissociated and suspended in Neurobasal medium supplemented with B27, 2 mM L-glutamine, Antibiotic/Antimycotic, 4 mg/ml Bovine Serum Albumin (BSA), 2 μg/mL heparin, 20 ng/mL recombinant epidermal growth factor (EGF) and 10 ng/mL basic fibroblast growth factor (bFGF). The number of primary neurospheres was counted and passaged after 7 days. To study proliferation, the third-passage neurospheres were

mechanically dissociated and cultured in the medium described above. To study differentiation, the mechanically dissociated neurospheres were plated in a poly-L-lysine-coated flask or chamber slides and cultured in Neurobasal medium (supplemented with B27, 2 mM L-glutamine and Antibiotic/Antimycotic solution) in the presence of 1% fetal bovine serum (FBS), heparin and bFGF. For the purposes of proliferation and differentiation evaluation, cells were cultured for 5 and 7 days, respectively, with and without melatonin supplied by Fagron Ibérica S.A.U. (Terrasa, Spain) in physiological (10 nM) and pharmacological (5-100 μM) concentrations.

2.3. Evaluation of neurosphere proliferation

NSC proliferation was evaluated by measuring the mean neurosphere diameter and with the aid of the 3-(4,5-dimethylthiazol-2-yl)-2,5-diphenyltetrazolium bromide (MTT) assay (Thermofisher Scientific, Madrid, Spain) involving the conversion of the water soluble MTT to an insoluble formazan. Briefly, the neurospheres were pelleted and mechanically dissociated, and the cells were then incubated with increasing concentrations of melatonin (0-100 μM) over a period of 5 days. The diameter of the neurospheres was calculated using light photography and image analysis using the ImageJ 1.46r software. For MTT assays, the medium was removed and replaced with a fresh medium without phenol red. The cells were then incubated with 1.2 mM MTT at 37°C for 4 hours and were subsequently incubated with SDS-HCl solution. Finally, the samples were mixed, and absorbance was read at 570 nm in a plate reader spectrofluorometer (Bio-Tek Instruments, Inc., Winooski, VT, USA).

To confirm the effect of melatonin on NSC proliferation, we also measured the percentage of Ki-67 positive nuclei. Briefly, after 5 days of treatment (10 nM and 25 μM melatonin) under proliferative conditions, the neurospheres were mechanically desegregated and deposited on a slide. Ki-67 expression was then determined by conventional immunocytochemistry using the Ki-67 antibody (Ab16667, 1:100; Abcam, Cambridge, United Kingdom). The Vectastain ABC kit (Vector PK6101; Burlington, NC, USA) was used

for qualitative identification of the Ki-67 protein, which was quantified using the Cell Counter plugin in ImageJ 1.46r software; the Ki-67 labeling index was based on the ratio of the number of Ki-67 stained cells to the total number of cells counted per section. At least 10 different randomly selected areas were counted using an Olympus CX41 microscope (Olympus, Hicksville, NY, USA).

2.4. Evaluation of neuronal differentiation

The effects of melatonin on NSC differentiation were evaluated using flow cytometry and confocal microscopy. Briefly, the neurospheres were mechanically dissociated and differentiated for 7 days in the presence of increasing concentrations of melatonin (0-100 μM). For the purposes of flow cytometry analysis, the cells were detached with the aid of 0.5% trypsin and were carefully fixed in suspension using 4% paraformaldehyde. For confocal microscopy analysis, the medium was washed, and the cells were fixed on slides with 4% paraformaldehyde. After fixation, in both cases, the cells were incubated with blocking/permeabilizing solution (0.1% Triton X-100, 5% BSA). The cells were then incubated overnight at 4°C with mouse primary anti-neuron-specific class III β-tubulin (TUJ1; MAB1195, 1:500, R&D, Madrid, Spain), anti-glial fibrillary acidic protein (GFAP; AF2594, 1:500; R&D), Nestin (MA1-110, 1:500, Thermofisher Scientific, Madrid, Spain) and oligodendrocytes (O4 clone 81; MAB 345, 1500, Millipore, Madrid, Spain). After several washes, we used goat anti-mouse IgG Alexa 488 (A11029, Life Technology, Carlsbad, California, USA) and goat anti-mouse IgG Alexa 594 (A11005, Thermofisher Scientific, Madrid, Spain) secondary antibodies to perform fluorescence labeling. For fluorescent microscopy purposes, nuclear staining was carried out using DAPI (1 μM). The fluorescent photomicrographs were taken with a Leica DMI6000 confocal microscope. Flow

cytometry analysis was performed with the aid of a Becton Dickinson FACSCanto II cytometer (Madrid, Spain).

2.5. Determination of melatonin by HPLC

Melatonin was extracted with trichloromethane, and the organic phase was evaporated to dryness (SPD 2010 Speed Vac System; Fisher Scientific, Madrid, Spain). The samples were analyzed by HPLC (Shimadzu Europe GmbH, Duisburg, Germany) with a Waters Sunfire C18 column (150 x 4.5 mm, 5 μm). The melatonin fluorescence was measured in a Shimadzu RF-10A XL fluorescence detector (Shimadzu Europe GmbH, Duisburg, Germany) with excitation and emission wavelengths of 285 nm and 345 nm, respectively [37].

2.6. Measurement of mitochondrial mass

To measure mitochondrial mass, we used Acridine Orange 10-nonyl bromide (NAO, Invitrogen), a metachromic dye which fluoresces at 533 nm; NAO binds to cardiolipin, a phospholipid specifically present on the mitochondrial membrane. We incubated 20,000 cells in 96-well plates with NAO (final concentration of 2.5 μM) at 37°C for 30 minutes in darkness. The cells were washed with PBS (PH 7.2) and re-suspended in no-phenol red medium. NAO fluorescence was measured in triplicate using the above-mentioned microplate reader (Ex/Em 485/538 nm).

2.7. Mitochondrial DNA quantification

Mouse mitochondrial DNA (mtDNA) was quantified by real-time PCR using a Stratagene Mx3005P Real-Time PCR System (Agilent Technologies, Inc., CA, USA) with the aid of primers and probes for the murine COXI gene (mtDNA) and mouse glyceraldehyde-3-phosphate dehydrogenase (nuclear DNA, nDNA) [38,39]. The mtDNA values were normalized by nDNA (mtDNA/nDNA ratio).

2.8. Quantification of CoQ9

Coenzyme Q9 (CoQ9) was extracted with 1-propanol. The samples were analyzed by HPLC (Gilson, Middleton, WI, USA), and the lipid components were separated with the aid of a

reverse-phase symmetry C18 column (3.5 μm, 4.6 × 150 mm; Waters, Barcelona, Spain). The electrochemical detector consisted of an ESA Coulochem III detector with a guard cell (upstream of the injector) at +900 mV and a conditioning cell at −600 mV (downstream of the column) followed by an analytical cell at +350 mV [40].

2.9. OXPHOS western blot analysis

Protein extraction and western blot analyses were performed as described in a previous study [39]. The antibodies used included an OXPHOS mouse antibody (MitoProfile Total OXPHOS Rodent WB Antibody Cocktail; 1:250; MS604; Mitosciences, Eugene, OR, USA) and a HRP goat anti-mouse IgG (1:1000; 554002; BD Pharmingen, San Jose, CA, USA). The proteins were visualized using a Western Lightning Plus-ECL chemiluminescence kit (PerkinElmer, Billerica, MA, USA) according to the manufacturer's protocol. The images were analyzed using image analysis station 2000R (Eastman Kodak Company, Rochester, NY, USA).

2.10. Mitochondrial membrane potential

5,5′,6,6′-tetracloro-1,1′,3,3′-tetraethyl-benzimidazolyl-carbocianine (JC-1) is a lipophylic cation which, in a reaction driven by membrane potential ($\Delta\psi_m$) in normal polarized mitochondria, assembles into a red fluorescence-emitting dimmer forming J-aggregates. However, the monomeric form present in cells with depolarized mitochondrial membranes

emits only green fluorescence. The ratio between red and green fluorescence is used as an index of mitochondrial membrane potential [41]. The cells were left untreated or were treated with 10 nM and 25 μM melatonin, as described above. They were then incubated for 15 min with JC-1 at 37°C, pelleted and suspended in PBS buffer without JC-1; the red/green fluorescence was analyzed at excitation/emission wavelengths of 550/595 nm and 485/530 nm, respectively, in a spectrofluorometer (Shimadzu, Duisburg, Germany). The green/red fluorescence ratio was normalized to μg of protein. Representative images were taken of each group treated.

2.11. Measurement of reactive oxygen species (ROS)

Following the change in fluorescence caused by the oxidation of 2′,7′-dichlorofluorescin diacetate (DCFH-DA), the levels of intracellular ROS were measured according to a method described in a previous study [42]. Once the dye entered the intracellular compartment, the acetate group on DCFH-DA was cleaved by intracellular esterases, thereby trapping the nonfluorescent DCFH. After being oxidized by ROS inside the cell, DCFH was converted into fluorescent DCF. The NSCs were seeded into a 96-well plate, washed with PBS and then incubated with 100 μm DCFH-DA in fresh medium at 37°C for 30 min. After removing excess DCFH-DA, the cells were washed again and incubated with Krebs-Ringer bicarbonate buffer containing 500 μm H_2O_2 to induce intracellular ROS. Fluorescence was measured every 5 min for 30 min at 485 nm excitation and 530 nm emission in a multiwell plate reader spectrofluorometer (Bio-Tek Instruments, Inc., Winooski, VT, USA). DCF fluorescence was normalized to protein content.

Measurement of GSH levels

Glutathione (GSH) was measured according to an established fluorometric method [43]. The cells were sonicated in ice-cold 50 mM Tris-HCl buffer (pH 7.4). After centrifugation at 800 g for 10 min at 4°C, the supernatant aliquots were deproteinized using 10% ice-cold trichloroacetic acid and centrifuged at 20,000 g for 15 min. The supernatant aliquots were incubated with an ortho-phthalaldehyde/ethanol solution (1 mg/mL) and phosphate buffer (100 mM sodium phosphate and 5 mM EDTA-Na2, pH 8.0) at room temperature for 15 min. The fluorescence of the samples was then measured at 340 nm excitation and 420 nm emission wavelengths in a plate-reader spectrofluorometer (Bio-Tek Instruments, Inc., Winooski, VT, USA).

2.12. Cell transplantation

The mice received 10 μL/g 10 μL/g of anesthetic, prepared from 37.5 μL Ketamine (Imalgine1000), 50 μL Meclotomidina (StartSedan) and 412.5 μL saline (0.9%). The mice

were then peeled off with scissors and placed in the stereotaxic device, while the head was kept as static and straight as possible. The skin was opened with a scalpel, and the bregma and lambda points were marked. The coordinates of the injection site were as follows: Parkinson (striatum): AP. +0.5 cm; ML: +0.15 cm; DV: +0.25 cm; Alzheimer (CA1 from hippocampus): AP: -0.25 cm; ML: +0.21 cm; DV: +0.18 cm. Then, a total volume of 5 μL of NSCs (10^6 cells for AD and 5 x 10^4 cells for PD) suspended in PBS was injected at an infusion rate of 0.5 μL/minute. After injection, the needle was left for 5 minutes before removal. The skin was then sutured, and betadine was applied. Finally, the same amount of atipamezole (StopSedan) than that of anesthesia was intraperitoneally injected.

2.13. Histological studies

The dissected brains were formalin-fixed and paraffin-embedded for sectioning. Multiple 4-µm-thick sections were deparaffinized with xylene and stained with H&E, Masson's TCM, PAS and LFB. Immunohistochemistry was carried out on these sections using the primary antibodies, rabbit anti-tyrosine hydroxylase (Millipore, AB152) and mouse anti-amyloid beta A4 protein, clone MM26-2.1.3 (Millipore, MAB8768). The Dako Animal Research Kit for mouse primary antibodies (Dako Diagnóstico S.A., Spain) was used to qualitatively identify antigens by light microscopy. The sections were examined at 40-400x with the aid of an Olympus CX41 microscope, and the images were scanned under equal light conditions using CELL A software (Olympus, Hicksville, NY, USA).

2.14. Statistical analysis

Statistical analyses were performed using GraphPad Prism 6 Scientific software (GraphPad Software, Inc., La Jolla, CA, USA). The data were expressed as the means ± SEM of a minimum of three independent experiments. One-way ANOVA and a *post hoc* Tukey test were used to compare differences between the experimental groups. The data were expressed as means ± SEM. A P value of <0.05 was considered to indicate statistical significance.

3. RESULTS

3.1. The effect of melatonin on NSC proliferation is dose-dependent

To determine the effect of melatonin on NSC proliferation, the neurosphere cultures were treated with increasing concentrations of melatonin (0-100 μM). The diameter of neurospheres was measured after 5 days of melatonin treatment to assess NSC proliferation. The diameter of neurospheres was unaffected at physiological concentrations of melatonin (10 nM), but significantly decreased at pharmacological concentrations of 25 μM and 100 μM (~272 μm as compared to ~186.5 and 183.2 μm, respectively) (Fig. 1A). MTT assays revealed that melatonin at pharmacological concentrations (5-100 μM) significantly reduced the proliferation of NSCs after 5 days as compared to the untreated control cells, while no changes were noted at physiological levels (10 nM melatonin) (Fig. 1B). As 10 nM and 25 μM of melatonin caused the weakest and strongest effect on cell proliferation, respectively, we decided to use these concentrations in further experiments. To confirm the effect of melatonin on cell growth, we disaggregated the neurospheres and measured the expression of proliferation marker Ki-67 using immunocytochemistry [44]. As expected, both untreated and 10 nM melatonin-treated cells presented similar Ki-67 reactivity levels (~35% and ~38%, respectively) after 5 days. However, 25 μM of melatonin was found to significantly reduce Ki-67 expression (~27%) **(**Fig. 1C**)**.

3.2. The effect of melatonin on NSC differentiation is dose-dependent

Given the effect of melatonin at pharmacological concentrations on cell proliferation, we sought to determine whether melatonin influences NSC differentiation. At a concentration of 25 μM, melatonin caused phenotypic changes associated with cell differentiation. As with neuronal cells, under differentiation conditions, the NSCs displayed refracted bodies with more elongated branches than control or 10 nM melatonin-treated cells **(**Fig. 2A**)**. We also determined whether melatonin exposure influences the expression of Nestin, Tuj-1, O4 or GFAP proteins under differentiation conditions. According to immunofluorescence imaging

and flow cytometry data, 25 μM of melatonin decreased the percentages of Nestin positive cells (~3%) as compared to control (~50%) or 10 nM melatonin-treated (~60%) cells, but significantly increased the percentage of Tuj-1 (~60%) and O4 positive cells (~18%) compared to the control (~11% and ~3%, respectively) and 10 nM melatonin-treated groups (~11% and 2%, respectively). Interestingly, melatonin did not modulate differentiation into GFAP-expressing astrocytes **(**Fig. 2B, C).

3.2. Melatonin levels in NSCs

To determine whether melatonin accumulates in cells according to its extracellular concentrations, we estimated indoleamine content. Using HPLC analysis, melatonin was found to accumulate in NSCs after 5 days of treatment; however, at the highest concentration (25 μM), a 2-fold increase in melatonin as compared to the lowest concentration (10 nM) was observed in cells (Fig. 3, red bars). A similar pattern was observed after 7 days of incubation in the differentiation medium (Fig. 3, blue bars).

3.3. Melatonin promotes mitochondrial morphology and mass modifications in NSC in a dose-dependent manner

Although the mechanisms of melatonin involved in NSC proliferation and differentiation are still poorly understood, mitochondrial function probably plays a role. Mitochondrial biogenesis has been linked to several physiological and pathological processes in the brain [45]. Interestingly, mitochondria have been suggested to be an intracellular target of melatonin [32]. Thus, using electron microscopy (EM), we evaluated the morphological effect of melatonin on mitochondria from NSCs and differentiated cells. Under proliferative conditions, the control cells displayed circular mitochondria with a limited number of cristae. After treatment with 10 nM melatonin, the mitochondria displayed a cristae development pattern similar to that in control cells. However, 25 μM melatonin modified the shape of mitochondria, including an elongated form with a large number of cristae **(**Fig. 4, proliferation**)**. Under differentiation conditions, all cells showed a mitochondrial structure

similar to that of NSCs treated with 25 μM melatonin, which is indicative of a more developed organelle (Fig. 4, differentiation). To confirm that these morphological changes truly reflect an increase in mitochondrial mass, we also measured this parameter with the aid of acridine orange. According to fluorescence data, 25 μM melatonin significantly increased mitochondrial mass in NSCs under proliferative conditions as compared to control and 10 nM melatonin-treated cells (Fig. 5A, red bars). These values are similar to those from cells under differentiation conditions (Fig. 5A, blue bars). The highest values for mitochondrial mass were observed in cells under differentiation conditions treated with 25 μM melatonin.

3.4. Melatonin promotes the up-regulation of mitochondrial DNA, CoQ9 and respiratory complexes in NSC in a dose-dependent manner

We next determined the levels of mtDNA in NSCs under both proliferative and differentiation conditions using real-time PCR. According to the mtDNA/nDNA ratio, neither control nor 10 nM melatonin treatments affected mtDNA levels in proliferative NSCs (Fig. 5B, red bars). However, 25 μM melatonin significantly increased mtDNA to levels similar to those of differentiating cells (Fig. 5B, blue bars). We also determined whether increased mtDNA levels were related to modulations in CoQ9 and mitochondrial complexes. According to the quantitative data, proliferative NSCs exposed to 25 μM melatonin raised CoQ9 levels (~1.4-fold) significantly as compared to control cells (Fig. 5C, red bars). Similarly, cells under differentiation conditions increased CoQ9 levels with respect to proliferative control NSCs (Fig. 5C, blue bars), although no differences were observed between melatonin and control treatments in this group. Next, given the significant increase in mtDNA and CoQ9 values caused by 25 μM melatonin treatment in proliferative NSCs, we evaluated the levels of respiratory complexes I, II, III and IV and ATPase. According to western blot quantification, 25 μM melatonin significantly increased the values of all mitochondrial complexes as compared to control and 10 nM melatonin-treated cells (Fig. 5D).

3.5. Melatonin promotes mitochondrial bioenergetics function in NSC in a dose-dependent manner

The findings described above prompted us to determine whether mitochondrial bioenergetics is also affected in cells exposed to melatonin under proliferative and differentiating conditions. To do this, we used a Seahorse Extracellular Flux Analyser which enables the oxygen consumption rate (OCR, mitochondrial respiration) to be measured. Under proliferative conditions, melatonin treatment increased the basal OCR, spare respiratory capacity (SRC) and ATP production, while it decreased the proton leak rate (Fig. 6A). Under differentiating conditions, all groups showed a higher basal OCR as compared to that observed under proliferative conditions. Interestingly, NSCs exposed to 25 μM melatonin showed the highest basal OCR, SRC and ATP synthesis, as well as the lowest proton leak rate (Fig. 6B).

We next determined whether melatonin alters $\Delta\Psi_m$ and ROS generation in NSCs under both proliferative and differentiation conditions. We also measured ATP levels using HPLC and evaluated $\Delta\Psi_m$ with the aid of JC-1 staining. The JC-1 ratios and fluorescent microscopy showed that 25 μM melatonin caused a ~1.5-fold increase in $\Delta\Psi_m$ with respect to control and 10 nM melatonin treatments under proliferative conditions (Fig. 7A,C, red bars). Likewise, 25 μM melatonin lead to a ~1.6-fold increase in $\Delta\Psi_m$ with respect to the control group under differentiation conditions (Fig. 7A, C, blue bars). Physiological concentrations of melatonin (10 nM) also increased $\Delta\Psi_m$ under differentiation stimulus conditions. We also evaluated the ATP/ADP ratio in cells exposed to physiological and pharmacological concentrations of melatonin. 10 nM and 25 μM of melatonin lead to a ~1.8- and ~1.9-fold increase, respectively, in the ATP/ADP ratio under proliferative conditions (Fig. 7D, red bars). Under differentiation conditions, all groups showed increased ATP/ADP ratios as compared to proliferative control cells (Fig. 7D, blue color). It is worth noting that the highest ATP values, which showed a 2.9-fold increase, were observed in cells exposed to 25 μM

melatonin under differentiation conditions. In addition, similar ATP/ADP ratios were observed in NSCs under proliferation conditions exposed to 25 μM melatonin and in control cells under differentiation conditions. It is interesting to note that these ATP data are in line with the results obtained by the SeaHorse analyzer (Fig. 6).

In conclusion, there are similar patterns in proliferation and differentiating conditions (Fig. 6A and 7A). However, under differentiating conditions, all groups showed a higher basal OCR as compared to that observed under proliferative conditions, cells under differentiation conditions treated with 25 μM melatonin showed a reverse pattern, compared with that of 10 nM melatonin. The apparent paradoxical effect of melatonin may depend of some slight changes in mitochondrial bioenergetics at 10 nM melatonin. Because we did not find changes in ATP production and proton leak, it is possible that at this dose, there exist a slight accumulation of protons in the intermembrane space leading to the small increase in the membrane potential.

Since high mitochondrial function is linked to high ROS production [11], we assessed ROS levels in cells under both proliferative and differentiation conditions. DCF fluorescence measurements showed that cells under proliferative conditions produced low levels of ROS, with similar results being obtained in all groups (Fig. 7E, red bars). As expected, the differentiation stimuli significantly increased ROS production, with a ~4-fold increase observed in all groups (Fig. 7E, blue bars). As ROS production did not increase in cells treated with 25 μM melatonin, we decided to measure GSH levels as an indicator of antioxidant status. Accordingly, 25 μM melatonin increased GSH levels under both proliferative and differentiation conditions (Fig. 7F). Furthermore, 10 nM melatonin increased GSH values under differentiating conditions.

3.6. Effects of NSCs pre-treated with melatonin and transplanted in Parkinson's and Alzheimer's diseases mice models

To further confirm the application of melatonin in NSC differentiation as a potential

therapy for PD and AD, we evaluated the effect of transplanting NSCs pre-treated with melatonin 25 μM in the mouse models of both diseases. In the PD model, the mice were divided into 4 groups: (i) vehicle-treated mice (control); (ii) MPTP-treated mice; (iii) MPTP-treated and NSC-transplanted mice; (iv) MPTP-treated and melatonin/NSC-transplanted mice. The presence of dopaminergic neurons was evaluated by TH-immunoreaction (Fig. 8A, B). MPTP-treated mice showed a significant reduction in dopaminergic neurons as compared to control mice. NSC-transplanted mice displayed increased TH-positivity as compared to MPTP mice, although these levels were statistically lower than those for the control mice. It is interesting to note that the transplantation of NSCs pre-treated with melatonin in PD mice led to a recovery in the dopaminergic population up to control levels. In the AD model, mice were divided into 4 groups: (i) vehicle-treated non-Aβ-expressing mice (control); (ii) vehicle-treated Aβ-expressing mice; (iii) Aβ-expressing and NSC-transplanted mice; (iv) Aβ-expressing and melatonin/NSC-transplanted mice. Aβ staining and quantification (Fig. 9A, B) showed that AD-transgenic mice significantly increased Aβ plaques as compared to control levels. NSC transplants in AD-transgenic mice showed decreased Aβ plaques compared to non-transplanted mice, although their levels were significantly higher than control. However, transplants of NSC pre-treated with melatonin in AD-transgenic mice decreased Aβ plaques to levels similar to those in control mice.

4. DISCUSSION

In this study, the effect of melatonin on the mitochondrial metabolic profile in neuronal precursors has, for the first time, been shown during proliferation and terminal differentiation. Previous studies have demonstrated that melatonin promotes NSC proliferation at low doses (e.g.1 μM) [26,46,47]. It has been recently reported that melatonin at 1 μM could act as a trophic factor, increasing proliferation in precursor cells mediated through the melatonin receptor (MT1) coupled to ERK/MAPK signaling pathways [48,49]. However, other studies show that higher concentrations of melatonin (25-100 μM) reduced NSC

proliferation [26,50]. Our results demonstrated that melatonin, at pharmacological concentrations (25-100 μM), reduced NSC proliferation and increased neural differentiation without influencing astroglial fate. These results are in line with the hypothesis that pharmacological (e.g. 25 μM), but not physiological (e.g. 10 nM), concentrations of melatonin have a potent modulatory impact on NSC proliferation and differentiation [46]. We also confirmed these results showing that melatonin, at pharmacological concentrations, promotes oligodendrocytic differentiation. However, recently it has been shown that melatonin at 0.05 and 0.5 μM concentrations significantly increases the percentage of oligodendrocytes in NSCs [51].

Our results, suggest that the mitochondrial metabolism does not play a major role at the NSC proliferation stage. However, studies of mitochondrial bioenergetics during neural progenitor cell development suggest that differentiation involves increased aerobic activity of NSCs, specifically in relation to mitochondrial mass, mtDNA copy number, electron transport chain capacity and NADH-generating enzyme activity [52,53]. Our findings clearly support the hypothesis that melatonin in pharmacological doses successfully potentiates this aerobic activity by targeting the mitochondria of NSCs (Fig. 4,5); indeed, our results imply that the effect of melatonin on mtDNA content is vital for the development of mitochondrial mass and the synthesis of respiratory complexes I, III, IV and V during the early stages of differentiation. In addition, we have confirmed that pharmacological doses of melatonin positively modulate the OCR in both proliferative NSCs and differentiated neurons, leading to an increment in $\Delta\Psi_m$ and ATP levels (Fig. 6, 7).

On the other hand, oxidative phosphorylation (OXPHOS) in the mitochondria accounts for the majority of ATP production in cells. However, OXPHOS is known to release free radicals derived from normal or anomalous mitochondrial function [11]. Interestingly, during neuronal differentiation, a switch to high levels of oxygen consumption occurs, leading to an elevation in the levels of ROS, which are believed to be prime precursor cells

for differentiation [54]. We show that ROS levels significantly increase in NSCs under differentiation conditions. Interestingly, despite the high OXPHOS activity induced by pharmacological doses of melatonin, as demonstrated by mitochondrial complexes, OCR, $\Delta\Psi m$ and ATP production, no exacerbation in ROS levels occurred due to melatonin as compared to the control group. On the whole, these data suggest that melatonin in pharmacological doses plays a dual role during NSC differentiation by potentiating OXPHOS while, at the same time, promoting ROS scavenging derived from exacerbated mitochondrial activity.

The transfer of novel cell replacement therapy strategies to a clinical setting is an attractive option for the treatment of neurodegenerative disorders [55,56]. Previous research showed that melatonin modulates amniotic epithelial cells-derived neural cells engraftment when transplanted into the injured spinal cord, thus promoting the successful neural restoration [57] and given the impact of melatonin in pharmacological doses on NSC differentiation, as a proof of principle, we histologically evaluated the effect of the transplantation of melatonin-treated NSCs in the brain tissue of PD and AD mice.

Our results show that in PD mice, the transplantation of these cells has a remarkable impact on dopamine neuron engraftment. Recently, it has been demonstrated that the successful engraftment of human-derived dopaminergic cells can alleviate not only motor, but also non-motor, cognitive and neuropsychiatric deficits seen in murine PD models [58]. However, the values for dopaminergic neurons recorded after transplantation of NSCs in models of PD, though statistically significant, are frequently very low compared to control groups [59]. The massive engraftment of TH^+ cells promoted by NSC treatment with pharmacological concentrations of melatonin would therefore contribute not only to generating neurons in the transplanted tissue, but also to triggering the mechanism which enables NSC-mediated functional recovery [60].

We also show that melatonin-treated NSC transplantation leads to a decrease in Aβ

production in transgenic mice and a recovery to the levels observed in control mice. Given these results, it is reasonable to infer that the therapeutic action of engrafted NSCs modifies the deleterious environment which contributes to AD pathology, probably by influencing the affected area through the release of diffusible factors. Indeed, previous studies have reported that NSCs display not only a wide range of trophic factors which restrain not only Aβ production but also tau phosphorylation and cell death [61-63].

In conclusion, we demonstrated that pharmacological doses of melatonin contribute to halting the NSC cell cycle while inducing massive differentiation into mature neurons. We also confirmed that melatonin promotes oligodendrocytic differentiation. Interestingly, the effect of high doses of melatonin is executed by a mechanism involving the premature development of mitochondrial structures accompanied by an increase in mitochondrial mass, mtDNA, CoQ9 and mtDNA-associated mitochondrial complex levels. Consequently, pharmacological doses of melatonin also increase basal and spare respiration capacity, thus facilitating an increment in $\Delta\Psi_m$ and ATP synthesis. Remarkably, the effect of melatonin on OXPHOS activity was not found to influence ROS production, most probably because of its impact on antioxidant sustenance by inducing GSH synthesis. Finally, the priming of NSCs with pharmacological doses of melatonin enhances cell engraftment in the brain of PD and AD mouse models, even though the evaluation of the effect of NSC transplantation on motor assays in environmental PD and cognitive status in AD mouse model will have to be performed. Therefore, these findings suggest that neural replacement, using NSCs combined with pharmacological doses of melatonin, may be become an effective tool in the regenerative treatment of neurological diseases (Fig. 10**)**.

ACKNOWLEDGMENTS

This study was partially funded by the following grants: SAF2009-14037 from the Spanish Ministry of Economy and Competitivity (MINECO), CB/10/00238 from the Carlos III Health Institute, GREIB.PT_2010_04 from the CEIBiotic Program of the University of Granada,

Spain, and CTS-101 from the Innovacion, Science and Business Council, Junta de Andalucía, Spain. The study was carried out within the framework of the 'Convenio Marco 206-2012' agreement between the University of Antioquia in Colombia and the University of Granada in Spain. MJ-Del-Rio and CV-P were supported by Colciencias grants #1115-657-740786 (contract 623-2014). MM-P and V-SM are associate researchers. MM-P is funded by the Colciencias, Enlaza-Mundos and AUIP mobility programs. VS-M was funded by the AUIP mobility program. Finally, we wish to thank Michael O'Shea for proofreading the paper.

REFERENCES

1. Kalia LV, Lang AE. Parkinson's disease. *Lancet.* 2015;386:896-912.
2. Bloom GS. Amyloid-beta and tau: the trigger and bullet in Alzheimer disease pathogenesis. *JAMA Neurol.* 2014;71:505-508.
3. Miller DB, O'Callaghan JP. Biomarkers of Parkinson's disease: present and future. *Metabolism.* 2015;64:S40-46.
4. Sperling RA, Aisen PS, Beckett LA, et al. Toward defining the preclinical stages of Alzheimer's disease: recommendations from the National Institute on Aging-Alzheimer's Association workgroups on diagnostic guidelines for Alzheimer's disease. *Alzheimers Dement.* 2011;7:280-292.
5. Fortin JM, Azari H, Zheng T, et al. Transplantation of defined populations of differentiated human neural stem cell progeny. *Sci Rep.* 2016;6:23579.
6. Jackson EL, Alvarez-Buylla A. Characterization of adult neural stem cells and their relation to brain tumors. *Cells Tissues Organs.* 2008;188:212-224.
7. Qin Y, Zhang W, Yang P. Current states of endogenous stem cells in adult spinal cord. *J Neurosci Res.* 2015;93:391-398.
8. Lim DA, Alvarez-Buylla A. The Adult Ventricular-Subventricular Zone (V-SVZ) and Olfactory Bulb (OB) Neurogenesis. *Cold Spring Harb Perspect Biol.* 2016;8: a018820
9. Azim K, Berninger B, Raineteau O. Mosaic Subventricular Origins of Forebrain Oligodendrogenesis. *Front Neurosci.* 2016;10:107.
10. Martino G, Pluchino S, Bonfanti L, et al. Brain regeneration in physiology and pathology: the immune signature driving therapeutic plasticity of neural stem cells. *Physiol Rev.* 2011;91:1281-1304.
11. Murphy MP. How mitochondria produce reactive oxygen species. *Biochem J.* 2009;417:1-13.
12. Xavier JM, Rodrigues CM, Sola S. Mitochondria: Major Regulators of Neural Development. *Neuroscientist.* 2015;22:346-358
13. Diaz-Castro B, Pardal R, Garcia-Flores P, et al. Resistance of glia-like central and peripheral neural stem cells to genetically induced mitochondrial dysfunction--differential effects on neurogenesis. *EMBO Rep.* 2015;16:1511-1519.
14. Kim HJ, Shaker MR, Cho B, et al. Dynamin-related protein 1 controls the migration and neuronal differentiation of subventricular zone-derived neural progenitor cells. *Sci Rep.* 2015;5:15962.
15. Claustrat B, Leston J. Melatonin: Physiological effects in humans. *Neurochirurgie.* 2015;61:77-84.

16. Tuli HS, Kashyap D, Sharma AK,et al. Molecular aspects of melatonin (MLT)-mediated therapeutic effects. *Life Sci.* 2015;135:147-157.
17. Luchetti F, Canonico B, Betti M, et al. Melatonin signaling and cell protection function. *Faseb j.* 2010;24:3603-3624.
18. Manchester LC, Coto-Montes A, Boga JA, et al. Melatonin: an ancient molecule that makes oxygen metabolically tolerable. *J Pineal Res.* 2015;59:403-419.
19. Reiter RJ, Mayo JC, Tan DX, et al. Melatonin as an antioxidant: under promises but over delivers. *J Pineal Res.* 2016;61:253-278.
20. Diaz-Casado ME, Lima E, Garcia JA, et al. Melatonin rescues zebrafish embryos from the parkinsonian phenotype restoring the parkin/PINK1/DJ-1/MUL1 network. *J Pineal Res.* 2016;61:96-107.
21. Tapias V, Escames G, Lopez LC, et al. Melatonin and its brain metabolite N(1)-acetyl-5-methoxykynuramine prevent mitochondrial nitric oxide synthase induction in parkinsonian mice. *J Neurosci Res.* 2009;87:3002-3010.
22. Gunasingh MJ, Philip JE, Ashok BS, et al. Melatonin prevents amyloid protofibrillar induced oxidative imbalance and biogenic amine catabolism. *Life Sci.* 2008;83:96-102.
23. Lee SH, Chun W, Kong PJ, et al. Sustained activation of Akt by melatonin contributes to the protection against kainic acid-induced neuronal death in hippocampus. *J Pineal Res.* 2006;40:79-85.
24. Kong X, Li X, Cai Z, et al. Melatonin regulates the viability and differentiation of rat midbrain neural stem cells. *Cell Mol Neurobiol.* 2008;28:569-579.
25. Sharma R, Ottenhof T, Rzeczkowska PA, et al. Epigenetic targets for melatonin: induction of histone H3 hyperacetylation and gene expression in C17.2 neural stem cells. *J Pineal Res.* 2008;45:277-284.
26. Sotthibundhu A, Phansuwan-Pujito P, et al. Melatonin increases proliferation of cultured neural stem cells obtained from adult mouse subventricular zone. *J Pineal Res.* 2010;49:291-300.
27. Acuna-Castroviejo D, Martin M, Macias M, et al. Melatonin, mitochondria, and cellular bioenergetics. *J Pineal Res.* 2001;30:65-74.
28. Acuna-Castroviejo D, Escames G, Rodriguez MI, et al. Melatonin role in the mitochondrial function. *Front Biosci.* 2007;12:947-963.
29. Acuna Castroviejo D, Lopez LC, Escames G, et al. Melatonin-mitochondria interplay in health and disease. *Curr Top Med Chem.* 2011;11:221-240.
30. Escames G, Lopez LC, Garcia JA, et al. Mitochondrial DNA and inflammatory diseases. *Hum Genet.* 2012;131:161-173.
31. Lopez A, Garcia JA, Escames G, et al. Melatonin protects the mitochondria from oxidative damage reducing oxygen consumption, membrane potential, and superoxide anion production. *J Pineal Res.* 2009;46:188-198.
32. Doerrier C, Garcia JA, Volt H, et al. Identification of mitochondrial deficits and melatonin targets in liver of septic mice by high-resolution respirometry. *Life Sci.* 2015;121:158-165.
33. Doerrier C, Garcia JA, Volt H, et al. Permeabilized myocardial fibers as model to detect mitochondrial dysfunction during sepsis and melatonin effects without disruption of mitochondrial network. *Mitochondrion.* 2016;27:56-63.
34. Al-Jarrah M, Obaidat H, Bataineh Z, et al. Endurance exercise training protects against the upregulation of nitric oxide in the striatum of MPTP/probenecid mouse model of Parkinson's disease. *NeuroRehabilitation.* 2013;32:141-147.
35. Jankowsky JL, Slunt HH, Ratovitski T, et al. Co-expression of multiple transgenes in mouse CNS: a comparison of strategies. *Biomol Eng.* 2001;17:157-165.
36. Lois C, Alvarez-Buylla A. Proliferating subventricular zone cells in the adult mammalian forebrain can differentiate into neurons and glia. *Proc Natl Acad Sci U S*

A. 1993;90:2074-2077.

37. Chahbouni M, Escames G, Venegas C, et al. Melatonin treatment normalizes plasma pro-inflammatory cytokines and nitrosative/oxidative stress in patients suffering from Duchenne muscular dystrophy. *J Pineal Res.* 2010;48:282-289.
38. Lopez LC, Akman HO, Garcia-Cazorla A, et al. Unbalanced deoxynucleotide pools cause mitochondrial DNA instability in thymidine phosphorylase-deficient mice. *Hum Mol Genet.* 2009;18:714-722.
39. Garcia-Mesa Y, Gimenez-Llort L, Lopez LC, et al. Melatonin plus physical exercise are highly neuroprotective in the 3xTg-AD mouse. *Neurobiol Aging.* 2012;33:1124.e1113-1129.
40. Lopez LC, Quinzii CM, Area E, et al. Treatment of CoQ(10) deficient fibroblasts with ubiquinone, CoQ analogs, and vitamin C: time- and compound-dependent effects. *PLoS One.* 2010;5:e11897.
41. Reers M, Smith TW, Chen LB. J-aggregate formation of a carbocyanine as a quantitative fluorescent indicator of membrane potential. *Biochemistry.* 1991;30:4480-4486.
42. Wang H, Joseph JA. Quantifying cellular oxidative stress by dichlorofluorescein assay using microplate reader. *Free Radic Biol Med.* 1999;27:612-616.
43. Hissin PJ, Hilf R. A fluorometric method for determination of oxidized and reduced glutathione in tissues. *Anal Biochem.* 1976;74:214-226.
44. Liang AC, Mandeville ET, Maki T, et al. Effects of aging on neural stem/progenitor cells and oligodendrocyte precursor cells after focal cerebral ischemia in spontaneously hypertensive rats. *Cell Transplant.* 2016;25:705-714.
45. Onyango IG, Lu J, Rodova M, et al. Regulation of neuron mitochondrial biogenesis and relevance to brain health. *Biochim Biophys Acta.* 2010;1802:228-234.
46. Moriya T, Horie N, Mitome M, et al. Melatonin influences the proliferative and differentiative activity of neural stem cells. *J Pineal Res.* 2007;42:411-418.
47. Tocharus C, Puriboriboon Y, Junmanee T, et al. Melatonin enhances adult rat hippocampal progenitor cell proliferation via ERK signaling pathway through melatonin receptor. *Neuroscience.* 2014;275:314-321.
48. Sotthibundhu A, Ekthuwapranee K, Govitrapong P. Comparison of melatonin with growth factors in promoting precursor cells proliferation in adult mouse subventricular zone. *EXCLI J*. 2016;15:829-841
49. Yu X, Li Z, Zheng H, et al. Protective roles of melatonin in central nervous system diseases by regulation of neural stem cells. *Cell Prolif*. 2017;50.
50. Fu J, Zhao SD, Liu HJ, et al. Melatonin promotes proliferation and differentiation of neural stem cells subjected to hypoxia in vitro. *J Pineal Res*. 2011;51:104-112.
51. Ghareghani M, Sadeghi H, Zibara K, et al. Melatonin increases oligodendrocyte differentiation in cultured neural stem cells. *Cell Mol Neurobiol*. 2016.
52. Chen CT, Hsu SH, Wei YH. Upregulation of mitochondrial function and antioxidant defense in the differentiation of stem cells. *Biochim Biophys Acta*. 2010;1800:257-263.
53. Agostini M, Romeo F, Inoue S, et al. Metabolic reprogramming during neuronal differentiation. Cell Death Differ. 2016;23:1502-15014.
54. Yanes O, Clark J, Wong DM, et al. Metabolic oxidation regulates embryonic stem cell differentiation. *Nat Chem Biol.* 2010;6:411-417.
55. Kriks S, Shim JW, Piao J, et al. Dopamine neurons derived from human ES cells efficiently engraft in animal models of Parkinson's disease. *Nature*. 2011;480:547-551.
56. Lee IS, Jung K, Kim IS, et al. Human neural stem cells alleviate Alzheimer-like pathology in a mouse model. *Mol Neurodegener*. 2015;10:38.
57. Gao Y, Bai C, Zheng D, et al. Combination of melatonin and Wnt-4 promotes neural

cell differentiation in bovine amniotic epithelial cells and recovery from spinal cord injury. *J Pineal Res.* 2016;60:303-312.
58. Lelos MJ, Morgan RJ, Kelly CM, et al. Amelioration of non-motor dysfunctions after transplantation of human dopamine neurons in a model of Parkinson's disease. *Exp Neurol.* 2016;278:54-61.
59. Zuo FX, Bao XJ, Sun XC, et al. Transplantation of Human Neural Stem Cells in a Parkinsonian Model Exerts Neuroprotection via Regulation of the Host Microenvironment. *Int J Mol Sci.* 2015;16:26473-26492.
60. Shen Y, Huang J, Liu L, et al. A Compendium of Preparation and Application of Stem Cells in Parkinson's Disease: Current Status and Future Prospects. *Front Aging Neurosci.* 2016;8:117.
61. Zhang H, Gao Y, Dai Z, et al. IGF-1 reduces BACE-1 expression in PC12 cells via activation of PI3-K/Akt and MAPK/ERK1/2 signaling pathways. *Neurochem Res.* 2011;36:49-57.
62. Hawryluk GW, Mothe AJ, Chamankhah M, et al. In vitro characterization of trophic factor expression in neural precursor cells. *Stem Cells Dev.* 2012;21:432-447.
63. Tuszynski MH, Thal L, Pay M, et al. A phase 1 clinical trial of nerve growth factor gene therapy for Alzheimer disease. *Nat Med.* 2005;11:551-555.

Figure Legends

FIGURE 1. Melatonin at pharmacological concentrations decreases the proliferation of NSCs. (A) Representative pictures of neurosphere size at different melatonin concentrations (aMT 0-100 μM). The images were obtained by phase contrast microscopy. Magnification, 200x; scale bar, 100 μm. The histogram indicates the mean diameter of neurospheres in all groups. (B) Bar graph of cell proliferation measurements at different concentrations of melatonin using MTT assays. (C) Immuno-cytochemical staining of cell proliferation marker Ki-67 and its percentage quantification. Magnification, 400x; scale bar, 50 μm. Data are presented as means ± SD. ***P<0.01* and ****P<0.001* as compared to the control group.

FIGURE 2. Melatonin at pharmacological concentrations promotes the differentiation of NSCs into neurons and oligodendrocytes**.** Cells under differentiation conditions were left untreated (control) or were treated with 10 nM and 25 μM melatonin (aMT) for 7 days. (A) Phase-contrast images showing morphological changes during neuronal differentiation. Magnification, 200x; scale bar, 50 μm. (B) Confocal microscopy immunofluorescence pictures showing the expression of neural stem cell (Nestin, red), mature neuronal (Tuj-1,

green), oligodendrocyte (O4, red) and astrocyte (GFAP, green) markers and DAPI (blue) nuclei staining. Magnification, 200x; scale bar, 50 μm. (C) Quantitative flow cytometry data showing percentage for each marker. Data are presented as means ± SD. **P<0.05,* ***P<0.01* and ****P<0.001* as compared to control group.

FIGURE 3. Intracellular melatonin increases after melatonin treatment in cells under proliferative and differentiating conditions. The figure shows the values for melatonin in cells under proliferative and differentiation conditions that were left untreated (control) or treated with 10 nM and 25 μM melatonin (aMT). Data are presented as means ± SD. **P<0.05,* ***P<0.01* and ****P<0.001* compared with proliferation control group. *#P<0.05* compared with 10 nM melatonin-treated group.

FIGURE 4. Melatonin induces morphological changes in mitochondria. Electron microscopy images of mitochondria in cells untreated (control) or treated with 10 nM and 25 μM melatonin (aMT) under proliferation and differentiation conditions. Swollen and less dense mitochondria are observed in proliferative cells without melatonin; more complex mitochondria are observed in differentiating cells. Scale bar 0.6 μm and 1 μm for proliferation and differentiation, respectively.

FIGURE 5. Pharmacological doses of melatonin promote mitochondrial function in cells under proliferative and differentiating conditions. (A) Fluorometric analysis of mitochondrial mass using NAO. (B) Determination of mitochondrial DNA content by RT-PCR. (C) HPLC analyses of coenzyme Q9 levels. Data are presented as means ± SD. **P<0.05 **P<0.01,* ****P<0.001* versus proliferation control group. (D-E) WB analysis and densitometric quantification of OXPHOS in NSC mitochondria. Data are presented as means ± SD. **P<0.05 **P<0.01, ***P<0.001* versus control, and *## P<0.01, ### P<0.001* versus 10 nM melatonin (aMT).

FIGURE 6. Melatonin improves mitochondrial respiration. Representative plots of oxygen consumption rate (OCR) profile, basal respiration, spare respiratory capacity, ATP production percentage and proton leak rate as determined by a Seahorse Bioscience XF Analyzer in cells under proliferation (A) and differentiation (B) conditions, untreated (Black color) or treated with 10 nM (red color) and 25 μM (blue color) melatonin (aMT). Arrows indicate time of addition of oligomycin (olyg), FCCP and rotenone/antymicin (Rot/Ant). Data are expressed as mean ± SD. *$P<0.05$ **$P<0.01$, ***$P<0.001$ versus control, and ### $P<0.001$ versus 10 nM melatonin.

FIGURE 7. Melatonin increases mitochondrial membrane potential and ATP levels without influencing ROS production. Representative fluorescence images of (A) proliferating cells and (B) differentiating cells, untreated or treated with 10 nM and 25 μM melatonin (aMT), stained with JC-1 probe (JC-monomer, -aggregates and merge). Magnification, 200x; scale bar, 50 μm. (C) Histograms showing the normalized ratio of red to green fluorescence intensity according to fluorescence spectrophotometer analysis. Data are presented as mean ± SD. *$P<0.05$, **$P<0.01$ and ***$P<0.001$ versus proliferation control. (D) ATP/ADP ratio under all conditions. (E) Intracellular ROS levels measured by fluorometry after staining with the DCF fluorescent probe. (F) GSH levels under all conditions. Data are presented as means ± SD. *$P<0.05$, **$P<0.01$ and ***$P<0.001$ versus proliferation control, and #$P<0.05$, ## $P<0.01$ versus the control in each cell group.

FIGURE 8. Transplantation of melatonin-treated NSCs improves neuronal restoration in the Parkinson's disease mouse model. (A) Striatal sections from all experimental groups were stained for TH to analyze the extent of the lesion and the survival of grafted cells. (B) Quantification of the immunoreactivity of graft-derived TH-positive cells. Data are expressed as means ± SD. (n = 2-3 per group). **$P < 0.01$ and ***$P < 0.001$. Scale bars and image

magnification: 1mm for 20x magnification (mag.); 500 μm for 40x mag.; 200 μm for 100x mag.; 50 μm for 400x mag.

FIGURE 9. Transplantation of melatonin-treated NSCs reduces Aβ plaques in the Alzheimer's disease transgenic mouse model. (A) Hipocampal sections from all experimental groups were stained for Aβ to analyze the extent of plaques and the effect of grafted cells. (B) Quantification of Aβ immunoreactivity. Data are expressed as means ± SD. (n = 2-3 per group). ***$P < 0.001$. Scale bars and image magnification: 500 μm for 40x magnification (mag.); 200 μm for 100x mag.; 50 μm for 400x mag.

FIGURE. 10. Hypothetical scheme of the effects of physiological and pharmacological doses of melatonin on neural stem cells (NSCs). (A) At physiological doses, NSCs have a less developed mitochondrial structure, including low levels of mtDNA and mitochondrial complexes. Low mitochondrial activity enables NSCs to be highly proliferative (large neurospheres), but are less differentiated after induction. (B) At pharmacological doses of melatonin, NSCs increase mitochondrial mass, mtDNA content and mitochondrial complex levels, thus facilitating an increment in $\Delta\Psi_m$ and ATP synthesis. Under these conditions, melatonin increases GSH levels and prevents ROS production. High mitochondrial activity promotes cell cycle reduction (small neurospheres) and induces substantial differentiation into mature neurons and oligodendrocytes, while maintaining basal glial cell levels. The treatment of NSCs with pharmacological doses of melatonin may enhance cell engraftment in the brain of PD and AD patients.

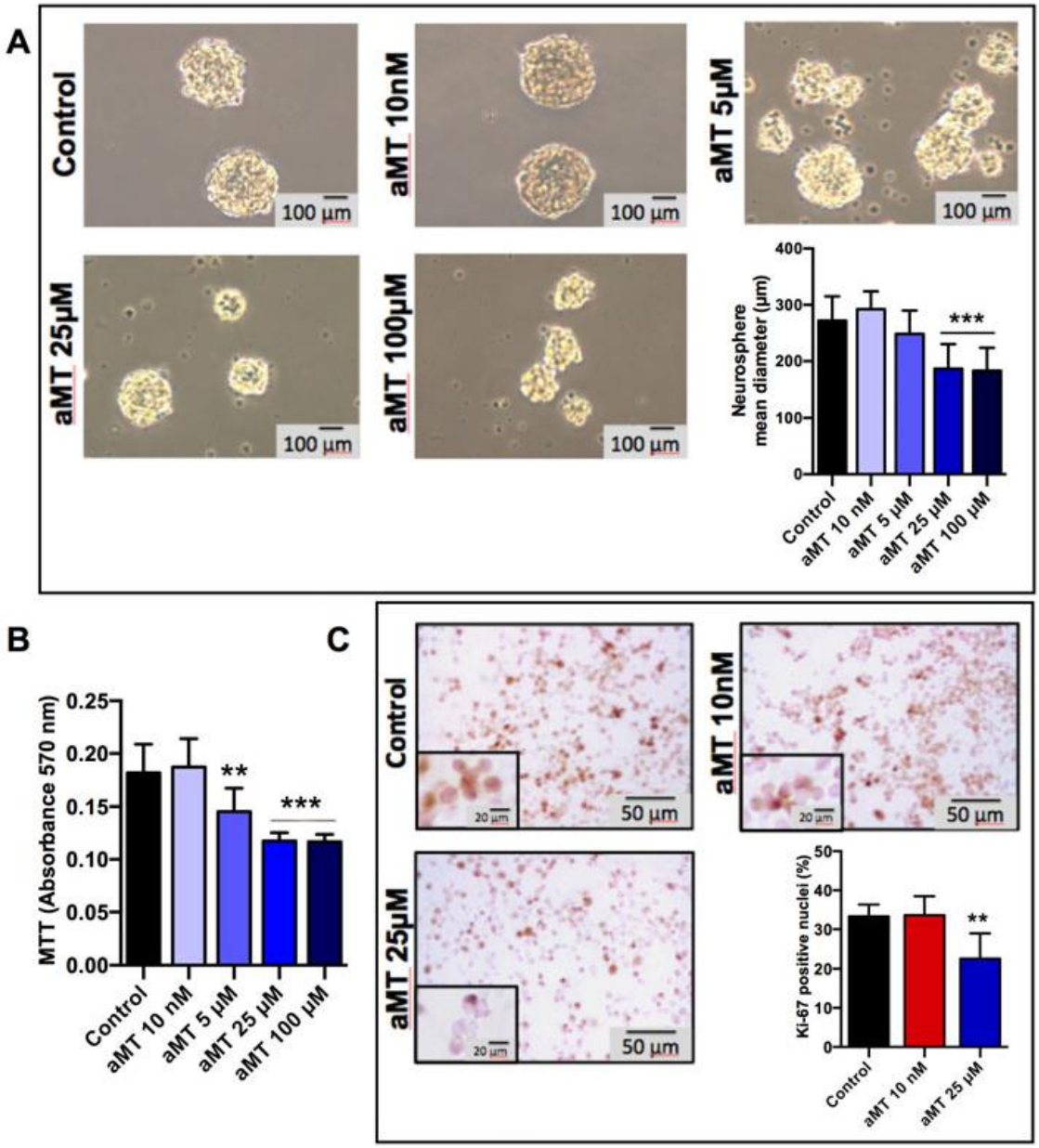
A
Control
aMT 10nM
aMT 5µM
aMT 25µM
aMT 100µM
100 µm
Neurosphere mean diameter (µm)
400
300
200
100
0
***
Control
aMT 10 nM
aMT 5 µM
aMT 25 µM
aMT 100 µM
B
MTT (Absorbance 570 nm)
0.25
0.20
0.15
0.10
0.05
0.00
**
***
Control
aMT 10 nM
aMT 5 µM
aMT 25 µM
aMT 100 µM
C
Control
aMT 10nM
aMT 25µM
20 µm
50 µm
Ki-67 positive nuclei (%)
50
40
30
20
10
0
**
Control
aMT 10 nM
aMT 25 µM

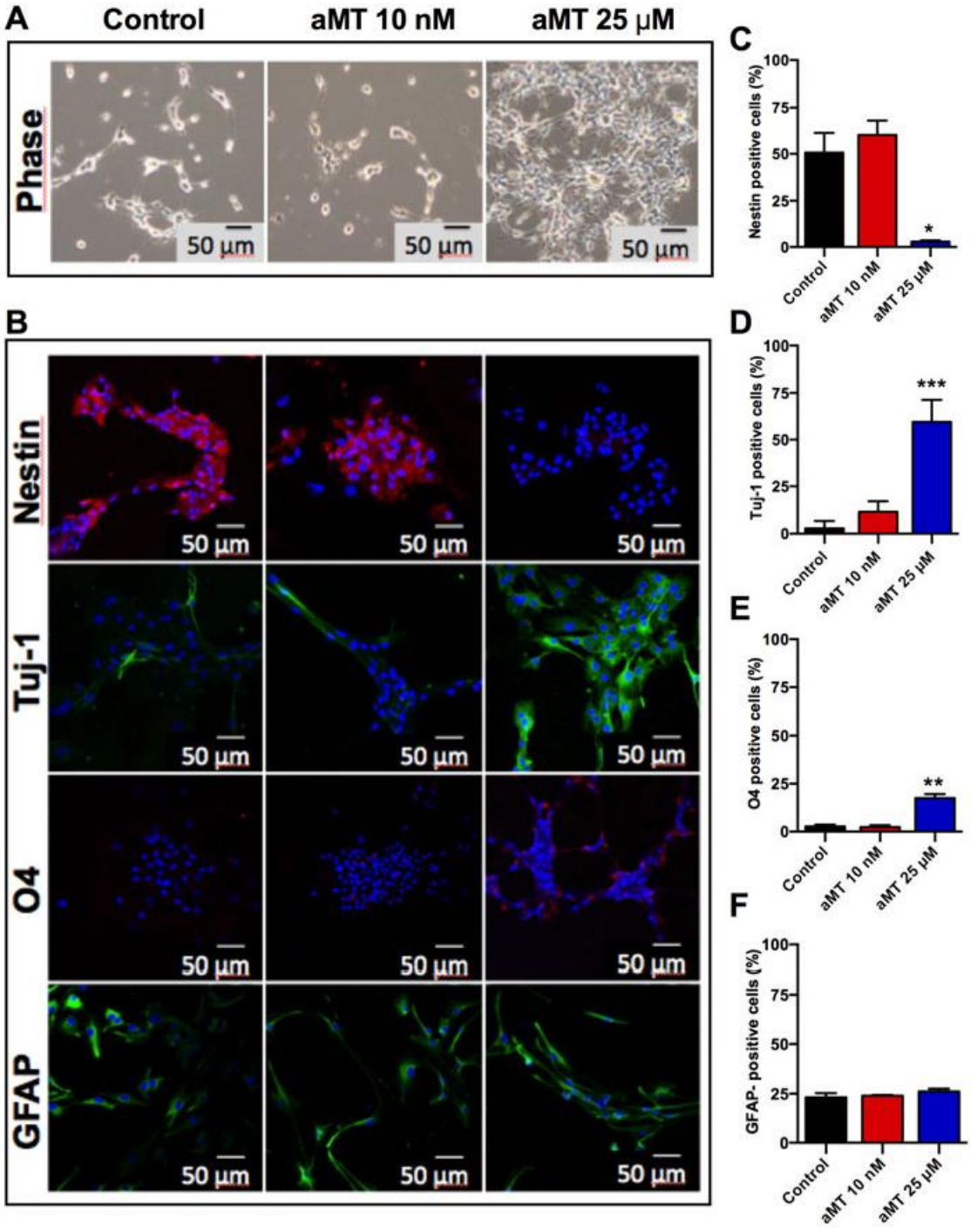
A
Control
aMT 10 nM
aMT 25 μM
Phase
50 μm
B
Nestin
Tuj-1
O4
GFAP
C
Nestin positive cells (%)
D
Tuj-1 positive cells (%)
E
O4 positive cells (%)
F
GFAP- positive cells (%)
Control
aMT 10 nM
aMT 25 μM
*
**
***

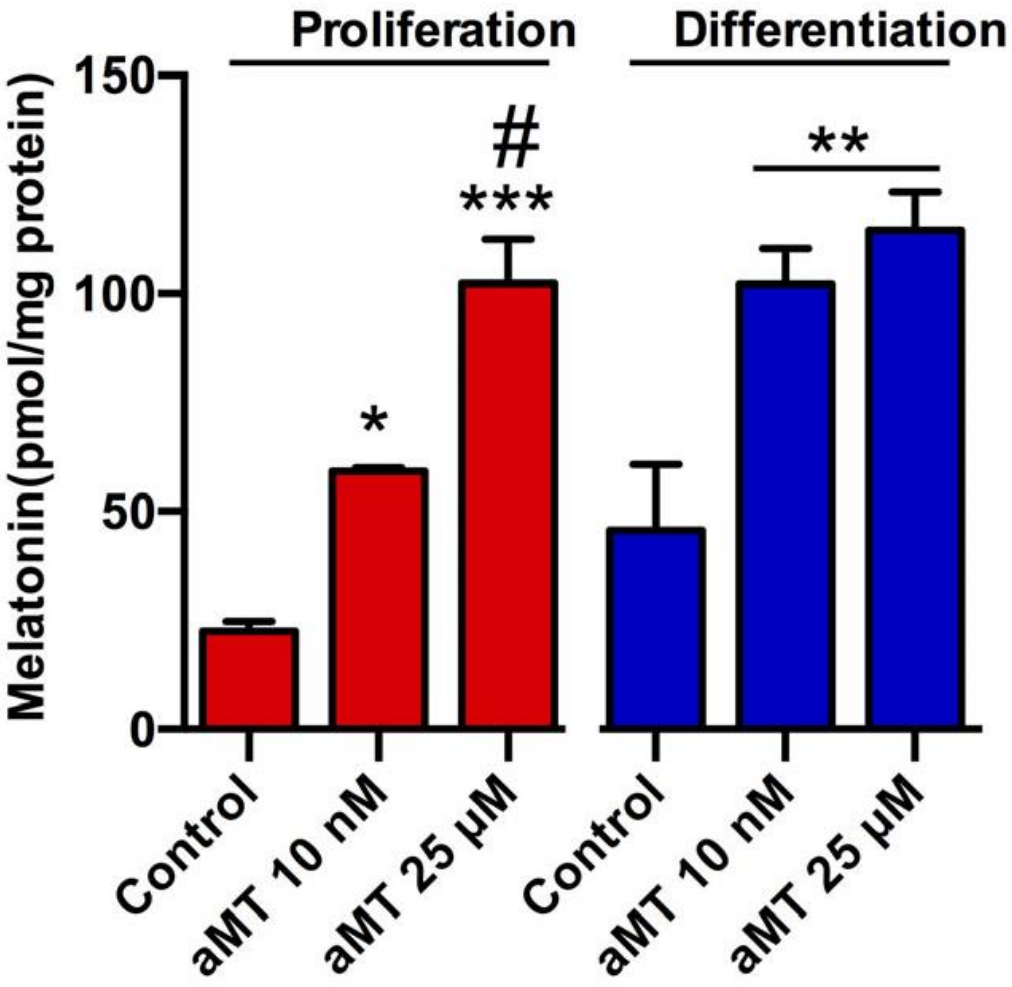
Proliferation
Differentiation
Melatonin(pmol/mg protein)
150
100
50
0
*
#
***
**
Control
aMT 10 nM
aMT 25 μM
Control
aMT 10 nM
aMT 25 μM

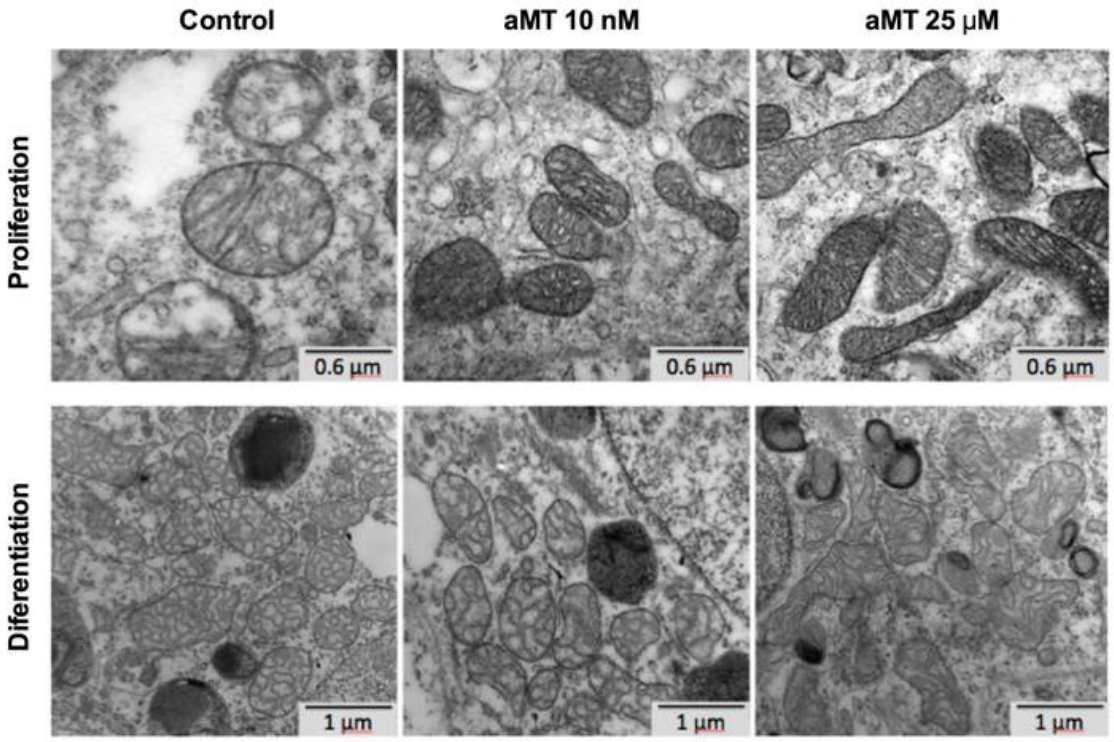
Control
aMT 10 nM
aMT 25 μM
Proliferation
Diferentiation
0.6 μm
0.6 μm
0.6 μm
1 μm
1 μm
1 μm

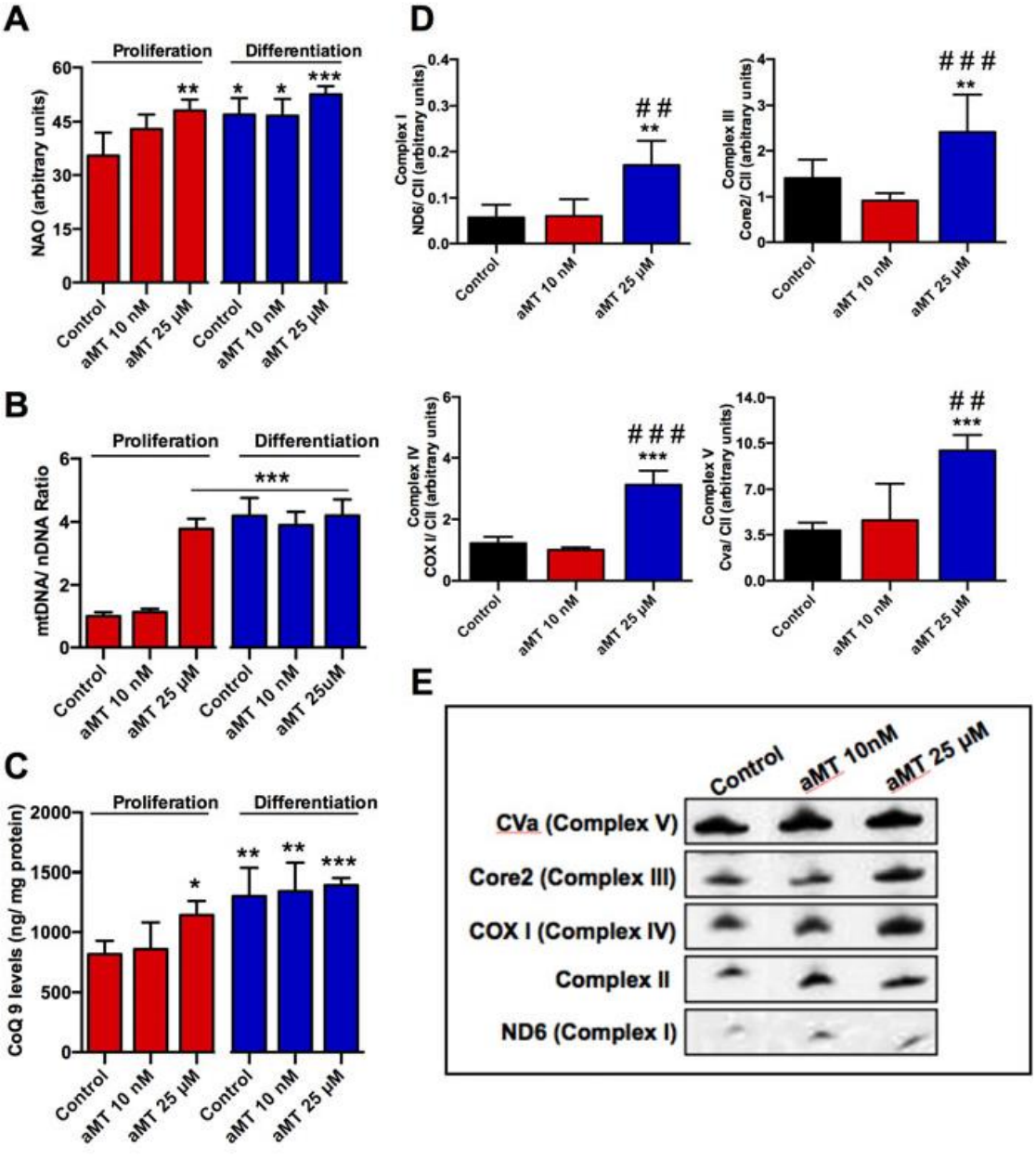
A
Proliferation
Differentiation
NAO (arbitrary units)
Control
aMT 10 nM
aMT 25 µM
B
mtDNA/ nDNA Ratio
aMT 25uM
C
CoQ 9 levels (ng/ mg protein)
D
Complex I
ND6/ CII (arbitrary units)
Complex III
Core2/ CII (arbitrary units)
Complex IV
COX I/ CII (arbitrary units)
Complex V
CVa/ CII (arbitrary units)
E
Control
aMT 10nM
aMT 25 µM
CVa (Complex V)
Core2 (Complex III)
COX I (Complex IV)
Complex II
ND6 (Complex I)

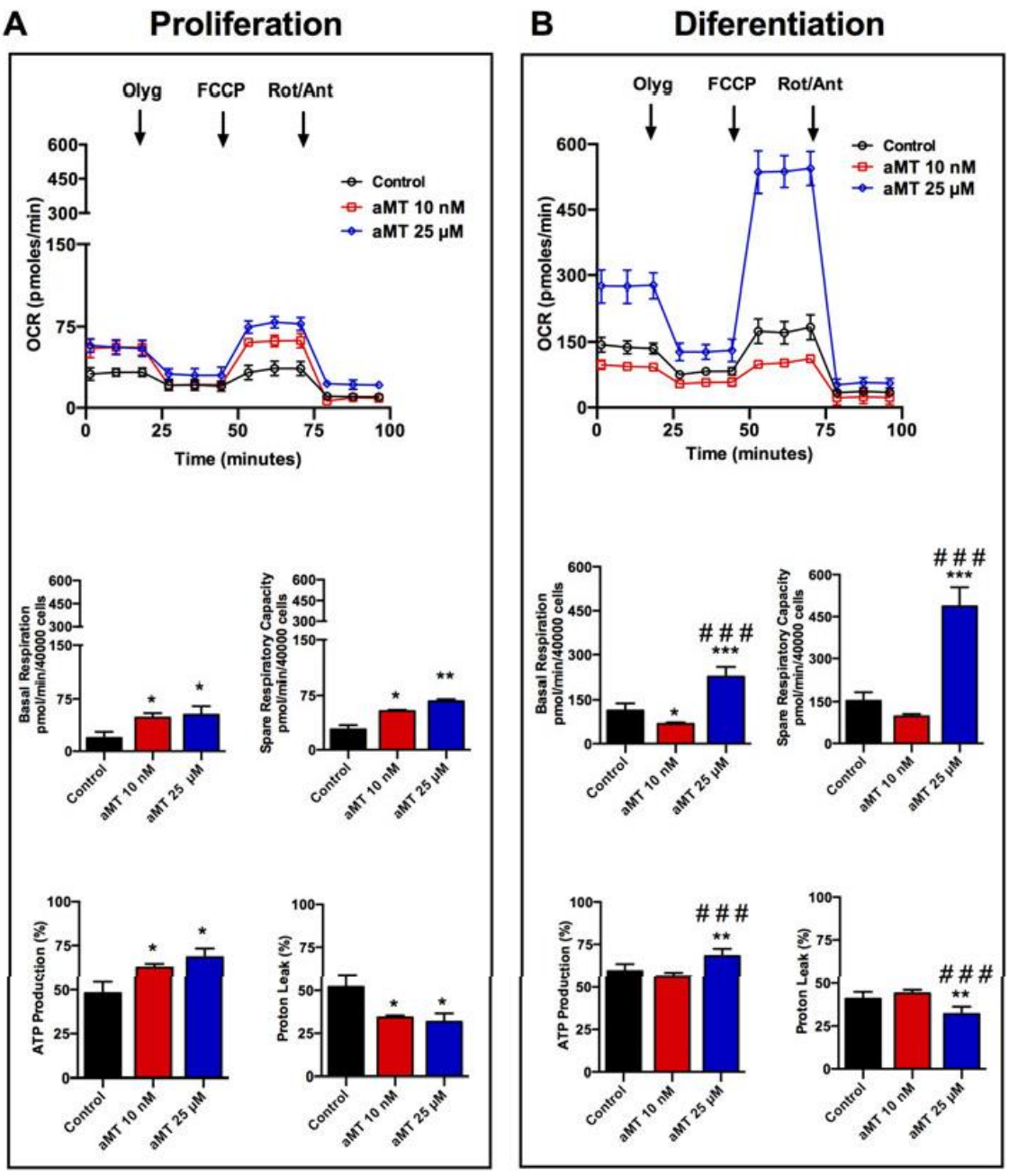
A
Proliferation
B
Diferentiation
Olyg
FCCP
Rot/Ant
Control
aMT 10 nM
aMT 25 µM
OCR (pmoles/min)
Time (minutes)
Basal Respiration pmol/min/40000 cells
Spare Respiratory Capacity pmol/min/40000 cells
ATP Production (%)
Proton Leak (%)
Control
aMT 10 nM
aMT 25 µM